1973

The design and calibration of a vibrating sample magnetometer

Donald Dwight Hoffman

THE DESIGN AND CALIBRATION OF A VIBRATING SAMPLE MAGNETOMETER

BY

DONALD DWIGHT HOFFMAN, 1946-

A THESIS

Presented to the Faculty of the Graduate School of the

UNIVERSITY OF MISSOURI-ROLLA

In Partial Fulfillment of the Requirements for the Degree

MASTER OF SCIENCE IN PHYSICS

1973

Approved by

Don M. Sparlin (Advisor) Wayne E. Tefft

W. J. James

ABSTRACT

The design and calibration of a vibrating sample magnetometer is described. The sample motion was in the direction of the external magnetic field which was produced by a superconducting solenoid. The maximum external magnetic field was 70 kilogauss. Sample temperature could be varied from $77^{\circ}K$ to $1000^{\circ}K$ with a vacuum jacketed furnace. The maximum temperature was obtained with approximately 27 watts. The instrument was calibrated to 1% with a spherical nickel sample.

ACKNOWLEDGEMENTS

The author wishes to thank his advisor, Dr. Don M. Sparlin, for suggesting this research problem and for his helpful advice and patient guidance during the course of this research. The author would like to thank Dr. William James of the Material Research Center, University of Missouri-Rolla, for the financial support provided for this research. He would also like to acknowledge the Physics Department staff and personnel who were most helpful during the course of this work.

TABLE OF CONTENTS

LIST OF FIGURES

I. INTRODUCTION

The magnetic susceptibility is one of the fundamental physical properties of magnetic materials. Many methods are used to measure this property with various degrees of accuracy. These methods can be divided into four major categories: null determination, indirect, force, and induction methods.

The null method[1] places the sample in a uniform magnetic field such that the sample does not affect the uniformity of the field, although the sample itself is uniformly magnetized. A cylindrical sample is wound with a fine wire coil through which a current is passed to restore the uniformity of the $\overline{B}$ field in all space. This current gives a direct measurement of the magnetization of the sample. Strong ferromagnetic materials and superconductors cannot be measured in this manner because of the large currents required in the coil.[2]

Indirect methods measure phenomena which indirectly involve the magnetic properties of materials. Common examples are measurement of the Faraday effect[3], analysis of galvanomagnetic effects such as the ferromagnetic Hall effect[4], and microwave ferromagnetic resonance measurements[5,6]. The general problem with indirect techniques is that they are limited to particular phenomena which are observable in a limited class of materials about which considerable prior knowledge is required. Indirect techniques are capable of very high sensitivity, however.

There are two principal types of force methods: the Curie[7] and the Gouy[8] methods. With the former the sample is subjected to an approximately constant $\overline{H} \cdot (d\overline{H}/dx)$. The production of such fields is generally accomplished by means of shaped pole faces in an electromagnet. This method requires an accurate knowledge of the value and the variation of a nonuniform field and of the position of the sample. Where relative measurements with respect to a standard sample are made, reproducible sample placement is the major problem.

The Gouy method uses a sample of sufficient length that its two ends are in substantially different fields. One end is in a uniform high field and the other end is in a much lower field. The cylindrical specimen has its axis in the y direction with the field in the x direction. The main advantage of this method is the insensitivity to the sample placement. Also, it is only necessary to measure a single uniform field. The disadvantages are the need for a long homogeneous sample of uniform cross section and the fact that variations in the magnetic properties that take place with small field increments cannot be measured.

The magnetic induction methods involve observation of the voltage induced in a detection coil, or coils, by flux changes arising from a change in the coil position, the sample position, or the applied magnetic field. Many different experimental arrangements have been developed to suit particular investigations. For the vibrating coil method (vibrating coil magnetometer) a laboratory magnet produces the external field in which a sample of magnetic

material is fixed. This type of magnetometer (developed by D. O. Smith[9,10]) drives the detection coil by a rod which passes through one of the magnet pole faces. The dipole field of the sample is detected as an ac electrical signal due to the coil vibrating along the axis of the dipole. The detection coil is kept far enough away from the sample to allow room for temperature or pressure generating apparatus. The difficulty with this magnetometer is that an extremely uniform applied magnetic field is required. It is difficult to correct for effects produced by small nonuniformities of the applied field, especially since these nonuniformities are functions of the applied field.

There are several experimental arrangements used with the vibrating sample magnetometer (VSM) in which the detection coil is fixed and the sample is moved. The direction of sample motion, parallel or perpendicular to the applied field, determines the geometry of the detection coils. With the direction of sample motion parallel to the axes of the detection coils and to the applied field, the detection coils can be symmetrically placed about the sample to obtain a maximum signal. Either the drive shaft passes through a hole in the pole face[11] or the parts moving parallel to the field fit between the pole faces of the electromagnet[12]. When the sample is oscillated perpendicular to the applied field, the detection coil configuration is such that the effective area-turns are asymmetrically distributed about the axis of sample vibration. In this case an oscillating quadrupole

field is observed. Foner[13] has described this type of magnetometer in great detail.

There are two major advantages to a superconducting magnet used as the source of the external field for a VSM, the extremely high field and the cylindrical geometry.[14] The magnetic field is parallel to the direction of sample motion permitting the detection coils to be placed symmetrically about the sample in the antiHelmholtz geometry. The drive red is easily passed through the core of the upper detection coil to place the sample in the center. While the VSM has been found to be one of the more operator compatible methods of magnetic measurement, it is not exempt from the systematic errors arising from magnetic image effects[15], sample shape[16], and mechanical vibrations.

Since temperature is an important thermodynamic variable in magnetic studies, its control must be incorporated in the experimental apparatus. The most common temperature control device[17] is the electric furnace. The furnace must fit into a relatively narrow space in the VSM as in most magnetization measurements. It is often necessary either to cool or to insulate the outside of the furnace to prevent heat from reaching the external magnet (the pole pieces or the solenoid), thus causing slow fluctuations of the magnetic field. With some experimental methods the temperature distribution in the furnace must be more uniform than in others. For example, the Guoy method requires a long furnace with a rather uniform temperature

distribution.

The availability of a superconducting solenoid suggested the selection of a VSM as the preferred method of measurement. A vacuum-jacketed furnace capable of raising sample temperature to $1000^{O}K$ was incorporated in the design. The purpose of this thesis is to describe that design and to present the calibration results for the instrument as it presently exists.

II. REVIEW OF LITERATURE

Measurements of magnetic properties are by now classic, but not until the 1950's was a VSM or VCM developed which had a high degree of accuracy. In 1951 Plotkin[18] described a VSM for use with a solenoid where the detection coil was coaxial with the magnetic field. Further development of the VSM was done by Foner[19] with different field and detection coil configurations. At the same time Smith[9] was working with a VCM. These instruments had several experimental difficulties in common. Continued work by Foner with the VSM resulted in a very versatile and sensitive instrument described in a detailed article in 1959[13]. That article was of principal importance in the development of the VSM reported in this paper. Two more recent articles[14,20] on the VSM and a bulletin[21] from Princeton Applied Research Corporation which produces a commercial VSM were of interest also.

One problem with a VSM is its calibration. Case[16] has evaluated two of the most widely accepted methods for calibrating a VSM, the comparison and the slope methods. In the former there are two important factors that must be considered: the shape of the sample and the magnetization of the standard. In the slope method the shape of the sample is important. It is convenient to use a spherical sample or at least an ellipsoidal sample for reasons made obvious in the Theory section. The production of spheres to a high degree of accuracy is an unavoidable experimental

problem which Cross[22] and Bond[23,24] have sucessfully explored.

Several reference books were most helpful to the design of this VSM. A book edited by Estermann[1] and a book by Bates[7] present general information on magnetism and its measurement. The design for the detection coils was taken from a book by Zijlstra[25].

III. THEORY

A. Magnetization of a Material

If any magnetic material is placed in a magnetic field, a dipole moment will be induced in the material. The energy of the dipole field depends in general on the magnetic induction, $\overline{B}$. The effects of the magnetic moment may well be described equally in terms of currents. It is useful, partly for historical reasons, to introduce the intensive variable magnetization, $\overline{M}$, defined as the magnetic moment per unit volume. In the presence of magnetizable matter

$$\text{curl } \overline{B} = 4\pi(\overline{J} + \overline{J}')/c. \tag{1}$$

$$\text{curl } \overline{B} = 4\pi\ \overline{J}/c + 4\pi\ \text{curl } \overline{M} \tag{2}$$

where $\overline{J}' = c\ \text{curl}\ \overline{M}$ may be thought of as a pseudo current. When $\overline{M}$ is constant, as within a uniformly magnetized material, the material has a pseudo current, $\overline{J}'$, only at its surface. A uniformly magnetized bar, for example, gives an induction $\overline{B}$ which is identical to that which would be produced by a solenoid consisting of a current sheet conforming to the geometry of the sides of the bar. Generally the relationship between $\overline{B}$ and $\overline{M}$ in materials is not quoted directly. Relationships are given between $\overline{M}$ and the magnetic field intensity, $\overline{H}$, where

$$\overline{H} = \overline{B} - 4\pi\ \overline{M}. \tag{3}$$

$\overline{H}$ is directly related to real currents by

$$\text{curl } \overline{H} = 4\Pi \overline{J}/c. \tag{4}$$

Since there are no sources of $\overline{B}$ in the sense of magnetic poles (div $\overline{B} = 0$), then

$$\text{div } \overline{H} = - 4\Pi \text{ div } \overline{M}. \tag{5}$$

Therefore, $\overline{H}$ is a vector which has sources in the sense of magnetic ples.

The free poles induced at the ends of a uniformly magnetized sample produce a demagnetizing effect. That is, the effect of magnetic polarization of the sample is to decrease the intensity of the magnetic field at a point which lies inside the sample by an amount which depends on $\overline{M}$ and the geometrical factor, N(called the demagnetizing factor). For a bar sample at points off the axis the calculation of the demagnetization field is extremely difficult. In the case of an ellipsoidal sample, the sample is uniformly magnetized in a uniform external field and the resulting surface current density varies in such a way as to make the calculation straightforward. Accordingly one can find an expression for N which is the same for all points within the specimen. For an ellipsoid of revolution with its long axis parallel to the field, Maxwell found[26]

$$N = (1/e^2 - 1)[1/2e \ln\{(1 + e)/(1 - e)\} - 1] \tag{6}$$

where the semi axes $a^2 = b^2 = (1 - e^2)c^2$.

The variables $\overline{B}$ and $\overline{M}$ will be uniform inside the ellipsoid placed in a uniform field regardless of the orientation of the axes with respect to the field. They coincide in direction only when one of the ellipsoid axes is aligned with the direction of the external field. (If there is an angle between $\overline{B}$ and $\overline{M}$, there is a torque on the sample.) When one of the axes of the ellipsoid coincides with the direction of the applied field, the magnetic induction within the sample is

$$\overline{B}_i = \overline{B}_o + 4\Pi(1 - N)\overline{M} \tag{7}$$

where $\overline{B}_o$ is the magnetic induction in the absence of the sample. The intensity of the magnetic field within the sample will also be uniform,

$$\overline{H}_i = \overline{B}_o - 4\Pi\ N\ \overline{M}. \tag{8}$$

Outside the sample $\overline{B}_o$ and $\overline{H}_o$ are equal although the sources must be considered as different. The induction, $\overline{B}_o$, will be a superposition of the fields from the solenoid producing the uniform external field and the pseudo or surface currents of the uniformly magnetized sample. The field intensity, $\overline{H}_o$, will be a superposition of the fields from the solenoid and the magnetic poles arising from div $\overline{M}$ at the surface of the sample.

A spherically shaped sample has the advantage among several

of being an ellipsoid of revolution. Since the semi axes are not uniquely defined for a spherical sample unless the material is anisotropic, $\overline{B}$ is always aligned with $\overline{M}$. The external field of a uniformly magnetized spherical sample is identical with that of a dipole of magnetic moment MV placed at the position of the center of the sphere. The fact that the external field depends only on MV and not the radius of the sphere means that an apparatus calibrated for a sphere of one radius is calibrated for all spheres. The demagnetizing factor for a sphere can be calculated from equation 6 with a = b = c which gives

$$N = 1/3. \tag{9}$$

B. Detection of the Magnetization

When a sample is placed in a uniform magnetic field and is forced to undergo sinusoidal motion, an ac electrical signal is induced in suitably placed stationary detection coils. This signal is proportional to the magnetic moment and to the amplitude and frequency of vibration. The external field of the sample is that of a stationary dipole plus an oscillating quadrupole field[13]. If the sample is translated in the direction of the uniform field, two stationary coils connected as an antiHelmholtz pair with the sample placed midway between them serve as the detection coil. An anti-Helmholtz pair generates a uniform gradient field which is optimum for detecting a sinusoidally translated dipole moment.

The calculation for the design of an antiHelmholtz pair of circular coils with a square winding cross-section has been presented

in reference 25. In this calculation there are three parameters: 1) the reduced half-width of the square winding cross-section (d), 2) the reduced half-distance between the coils (Z), and 3) the average coil radius (p). Two of the parameters must be arbitrarily selected. For example, the radius and the width of the coils may be limited by other factors. The separation of the coils is determined then by the calculation. In the reference the three parameters are plotted as Z/p versus d/p. Once d and p are selected, Z/p can be read directly.

The frequency and amplitude dependence of the induced voltage in the detection coil may be eliminated by means of a feedback system, or magnetization bridge. One such system is composed of an antiHelmholtz pair of coils (gradient coil) and a single reference coil. The pair of coils produce a gradient field which is detected by the reference coil undergoing sinusoidal motion at the same frequency and amplitude as the sample. The reference coil signal is subtracted from the detection coil signal and the resulting signal is fed into an amplifier. The amplifier converts the ac signal to a dc voltage which is fed-back to the gradient coil, thus forming a magnetic moment bridge. The dc voltage is then directly proportional to the magnetic moment of the sample if the gain of the amplifier and the geometrical factors of the antiHelmholtz coils are large enough. This proportionality is demonstrated by the following derivation. We can write for the detection coil voltage

$$V_m = g_m N_m A_m af(MV) = K_1 af(MV) \tag{10}$$

where: g_m = geometrical factor

N_m = number of turns on detection coil

A_m = area of detection coil

a = amplitude of vibration

f = frequency of vibration

MV = magnetic moment of sample

$K_1 = g_m N_m A_m$, a constant

V_m = voltage in detection coil.

And for the reference coil we can write

$$V_r = g_r N_r A_r afI_g = K_2 afI_g \tag{11}$$

where: g_r = geometrical factor

N_r = number of turns in reference coil

A_r = area of reference coil

I_g = current in gradient coil

V_r = voltage in reference coil.

The voltage output of the signal amplifier is

$$V_o = G(V_m - V_r) = G(K_1 afMV - K_2 afV_o/R) \tag{12}$$

where G is the gain of the amplifier and R is the series resistance of the gradient coil and feedback resistor. Solving for V_o we then have

$$V_o = GK_1afMV/(1 + GafK_2/R). \tag{13}$$

If the factor $GafK_2/R$ is much greater than one, then

$$V_o = (MV)K_1R/K_2. \tag{14}$$

The factor RK_1/K_2 (a constant) is determined by calibration.

C. Calibration of a Magnetometer

No matter how well designed a magnetometer is, its ultimate accuracy depends on the calibration technique. The two calibration methods most often used are the comparison and the slope methods. With the former the known saturation magnetization of a material is compared to the voltage generated in the detection coil be a vibrating spherical sample of the material. The voltage generated is proportional to the magnetization of this standard sample.

$$V_s = (4\pi M_s)Kd_s^3 \tag{15}$$

where: V_s = voltage induced in detection coil

M_s = known magnetization of standard sample

d_s^3 = volume of standard sample

K = proportionality constant

In the literature the saturation magnetization is usually given in gauss, hence the 4π factor. The calibration constant, K, is then

$$K = V_s/(4\pi M_s)d_s^3. \tag{16}$$

The unknown magnetization, M_o, of a sample is given in terms of the voltage generated in the detection coil by the sample, V_o, the volume of the sample, d_o^3, and the calibration constant, K.

$$4\Pi M_o = V_o/Kd_o^3. \tag{17}$$

Substituting for K gives

$$4\Pi M_o = (4\Pi M_s)(V_o/V_s)(d_s/d_o)^3 \tag{18}$$

where d_s and d_o refer to the diameter of the respective samples.

The three sources of error generated by this method are in the 1) magnitude of the standard magnetization, 2) ratio of the diameters, and 3) ratio of the voltages. Since the cube of the diameter ratio appears highly spherical samples must be ground. It is possible to grind spheres that are only 0.2% out of round or better. The percentage out of round is defined as

$$\frac{100(\text{max diameter} - \text{min diameter})}{\text{min diameter}} . \tag{19}$$

The average diameter of the spheres may be determined by 20 to 30 random measurements or by mass and density measurements.

Repeatability of the voltage readings is of great importance. Since two samples are used in the comparison technique for calibration, it is necessary to obtain reproducible sample positioning. The required positioning can be accomplished by varying the position of the detection coil or by varying the sample

position relative to the detection coil to obtain a maximum voltage reading. When using a superconducting magnet, the detection coil is not readily accessible for adjustment. In this case the positioning is accomplished by varying the sample position. This is a variation in one direction only, that of oscillation. By proper design of the detection coil the sample position in the coil can vary as much as 4 mm to either side of its midpoint with little change in the maximum voltage reading. Any motion perpendicular to the coil axis must be minimized in the design. Adjustment of this degree of freedom is not readily accomplished during measurements: sample motion perpendicular to the coil axis is minimized by allowing minimum separation between the sample holder and the inside wall of the magnetometer.

A source of error associated with the output voltage reading is due to detection coil motion in the external field. This can be reduced by affixing the coils firmly to the magnetometer and then placing spring fingers between the magnetometer and the inside wall of the superconducting magnet. The magnetometer must be firmly attached to the magnet support framework for minimum vibration noise in the detection coil. Any motion of magnetizable material near the detection coil will induce a voltage. Hence, the sample holder and driving rod must be nonmagnetic in the vicinity of the detection coil.

A source of systematic error is the induced current or magnetic image effect. The image effect results from the fact that when a

magnetic material is placed near a highly permeable medium, an image magnetic moment is induced in that medium. In a superconducting magnet, the signal due to the magnetic image is somewhat dependent on the past history of the solenoid, on the trapped flux, and on the fluxon distribution. The image effect is included in the calibration constant as a sort of demagnetization factor.

The saturation magnetization of the standard sample, normally pure nickel or iron, must be known when using the comparison method of calibration. There are variations in the reported values of the saturation magnetization of even the best known standards. Usually the value is given in emu per gram, and it is difficult to convert these values to $4\Pi\ M_s$ in gauss with accuracy. There is also the problem of not knowing if the standard sample is of the same composition and is being measured under the same conditions as were the samples whose values are reported. The magnetization of a sample will depend upon the purity, density, magnetic field, temperature, and state of annealing. All of these factors must be considered when selecting a standard sample.

With the slope method the instrument is calibrated from the initial slope of the magnetization curve of a spherical sample of high permeability. The voltage induced in the detection coil is a linear function of the applied field over the lower region of the magnetization curve. The relationship between $\overline{M}$ and the internal field, $\overline{H}_i$, of a material in the demagnetized state is defined as[27]

$$\overline{M} = (\mu - 1)\overline{H}_i/4\Pi \tag{20}$$

where μ is the relative permeability. Substituting equation 8 into equation 20 and solving for 4Π M (dropping the vector notation) gives

$$4\Pi\ M = H_o[(\mu - 1)^{-1} + N]^{-1} \tag{21}$$

where N is the demagnetizing factor. We rewrite this equation for the calibrating sample as

$$4\Pi\ M_c = H_c[(\mu - 1)^{-1} + N]^{-1}. \tag{22}$$

From equation 15 we can write

$$\Delta V_c = Kd_c^3\ \Delta(4\Pi\ M_c). \tag{23}$$

This can be resritten as

$$\Delta V_c = Kd_c^3[(\mu - 1)^{-1} + N]^{-1}\ \Delta H_c. \tag{24}$$

Solving for K gives

$$K = [(\mu - 1)^{-1} + N]\Delta V_c/d_c^3\ \Delta H_c. \tag{25}$$

Then substituting K into equation 17 gives the unknown magnetization of a sample as

$$4\pi M_o = V_o(d_c/d_o)^3[(\mu - 1)^{-1} + N]^{-1}(\Delta V_c/\Delta H_c)^{-1} \qquad (26)$$

where:

d_c = diameter of calibrating sphere

d_o = diameter of sample sphere with unknown magnetization

V_o = voltage due to sample with unknown magnetization

μ = relative permeability of calibrating sample

N = demagnetizing factor of calibrating sample

ΔH_c = change in the magnetic field applied to calibrating sample in linear portion of curve

ΔV_c = change in coil voltage from calibrating sample corresponding to ΔH_c.

The problems with the accuracy of the voltage and diameter measurements have already been pointed out. The three remaining values in equation 26 are the permeability, the demagnetizing factor, and the field H_c used in determining the slope $\Delta V_c/\Delta H_c$. The comparison of the two calibration methods is then a comparison of the accuracy with which we can determine μ, N, and H_c to that of $4\pi M_s$ of the standard sample.

The measurement of H_c should be no problem. The manufacturer usually supplied calibration data for the magnet. If one wants superior accuracy of calibration data, a nuclear resonance gaussmeter, in conjunction with a frequency counter, may be used to measure H_c with negligible error. The slope, $\Delta V_c/\Delta H_c$, should

be taken at several values of H_c to be sure that the linear portion of the curve is being used. If a material of high permeability is used, the value of $(\mu - 1)^{-1}$ is very small compared with the demagnetizing factor, N, for a sphere. The advantage of this slope method is the fact that it is not necessary to know μ accurately if it is sufficiently high. Any deviation from a true sphere causes an error in N which practically causes the same percentage error in M_o. Case[28] conducted experiments along this line to determine the accuracy in N. He concluded that the calibrating spheres should not be out of round more than approximately 0.1 percent. He also found that the error due to sample volume determination is actually greater than that due to misorientation of the sample. The total error expected from H_c, μ, and N terms should be less than a few tenths of a percent. This result in conjunction with the 0.1 to 0.2 percent possible error in the voltage and diameter terms, Case claims, makes it possible to expect errors of less than 0.5 percent with the slope method.

Making use of equation 21, one can combine the two methods for rapid estimation of the saturation magnetization. For example, using an iron or nickel sample, a curve is obtained as shown in Figure 1. By extrapolating the slope and the saturation magnetization line, the value H_s is obtained. The applied field H_s is that at which $4\pi M$ is equal to the saturation magnetization. Substituting H_s into equation 21 and assuming that μ is very large gives

$$4\pi M_s = H_s/N. \tag{27}$$

Hence H_s/N can be compared immediately to a literature value for the saturation magnetization of the sample.

Figure 1. Magnetization Versus External Magnetic Field

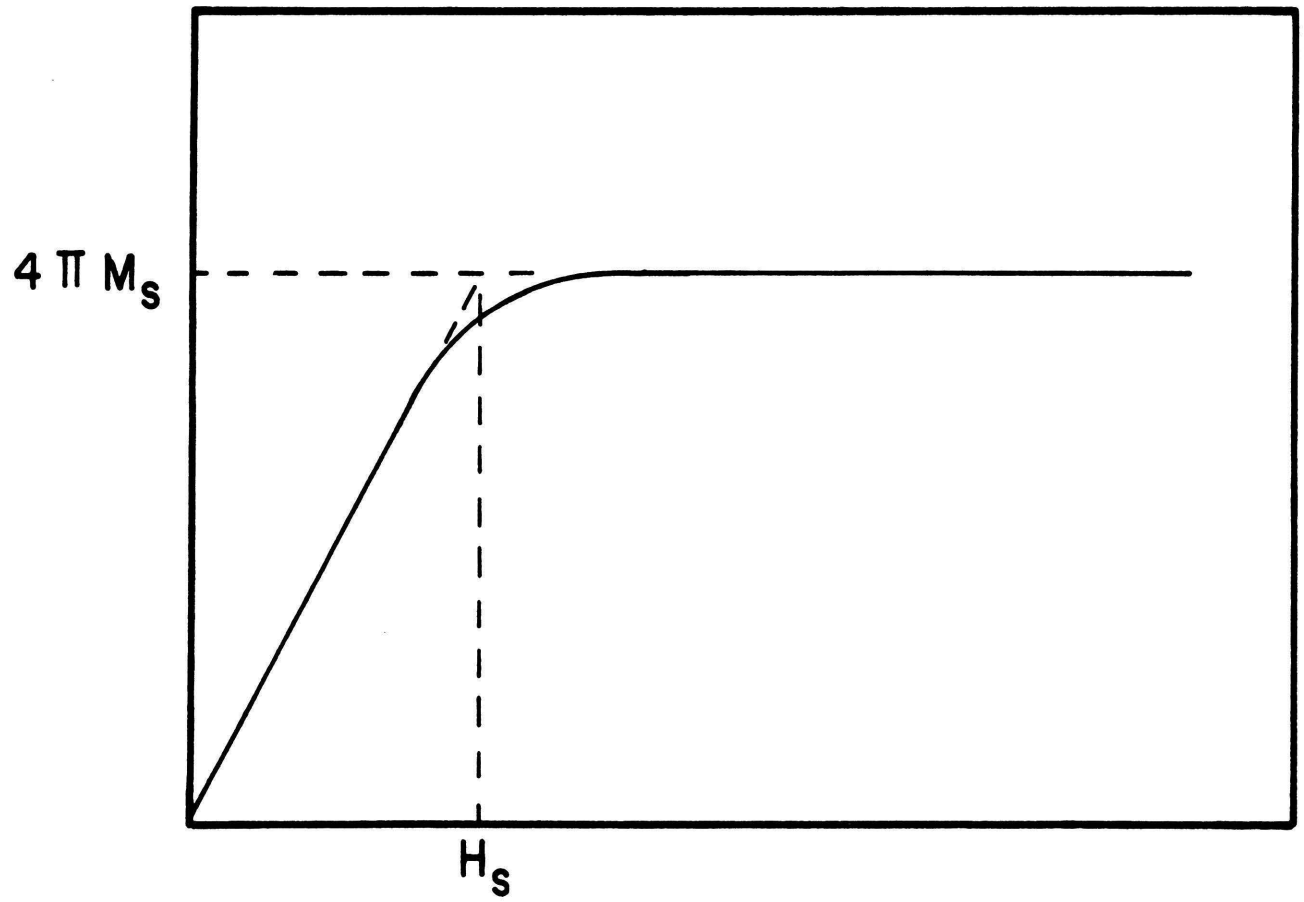

Figure 1

IV. MAGNETOMETER DESIGN

A simplified block diagram of the magnetometer is shown in Figure 2. The four basic elements of the magnetometer are the head, the drive rod and sample mount, the vacuum furnace, and the detection coil. The fifth basic element (not shown in the figure) is the electronics. Each of the basic elements of the magnetometer is described in detail in the following paragraphs.

A. Magnetometer Head

Figure 3 is a detailed drawing of the head in which the various parts are lettered to assist in the verbal description. The stainless steel can (A) was welded to the stainless steel rim (B) to form the vacuum tight cover of the magnetometer head. The stainless steel base plate (C) was tapped for six 6-32 screws (D) and was machined for an 'O'-ring vacuum seal (E). The cover was fastened to the base plate by the 6-32 screws and was vacuum sealed to the base plate by the'O'-ring. The base plate has a hole at its center into which a hollow cylindrical brass sleeve (F) was silver soldered. Three 1/4-20 bolts (G) equally spaced on a 3 inch bolt circle were silver soldered to the bottom of the base plate. A brass plate (H) with 1/4-20 body relief holes on the same 3 inch bolt circle was silver soldered to a hollow cylindrical brass sleeve (I). The sleeve (I) makes an 'O'-ring seal inside the brass sleeve (F). The three 1/4-20 bolts (G) pass through the corresponding holes in the plate (H). The plate (H) was held rigid with respect to the base plate by nuts on the bolts

Figure 2. Schematic Cross-Sectional View of Magnetometer

1. Vibration Generator
2. Gradient Coil
3. Reference Coil
4. Drive Rod
5. Detection Coil
6. Vacuum Furnace
7. Sample Mount
8. Superconducting Solenoid
9. Outer Vacuum Jacket

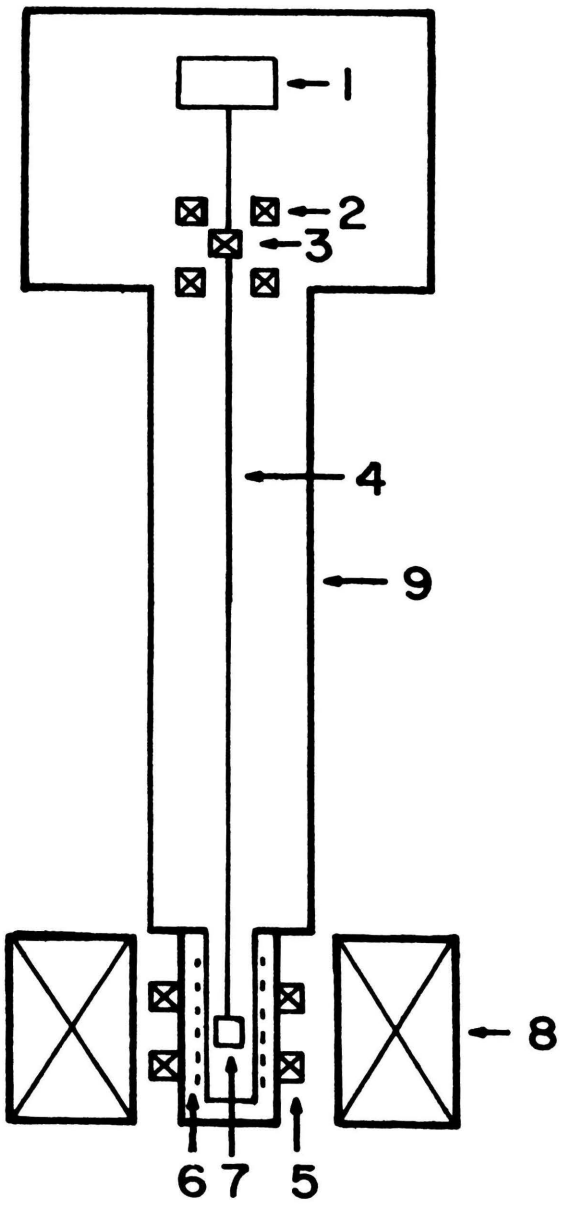

Figure 2

Figure 3. Schematic Cross-Sectional View of Magnetometer Head

A. Stainless Steel Can

B. Stainless Steel Rim

C. Stainless Steel Base Plate

D. 6-32 Screws

E. 'O'-Ring Vacuum Seal

F. Brass Sleeve

G. 1/4-20 Bolts (Sample Position Adjustment)

H. Brass Plate

I. Brass Sleeve

J. Ladish Triclover Flange

K. Vacuum Line to Inside of Magnetometer

L. Electrical Feed-Through

M. Electrical Feed-Through

N. Vacuum Line to Furnace

O. Electrical Lead Tube for Furnace

P. Electrical Lead Tube for Detection Coil

Q. Furnace Support Tube

R. Vibration Generator

S. Drive Rod Support

T. Gradient Coil Assembly

U. Reference Coil Assembly

V. Drive Rod

W. 1/4-20 Brass Bolts (Vibration Generator Support)

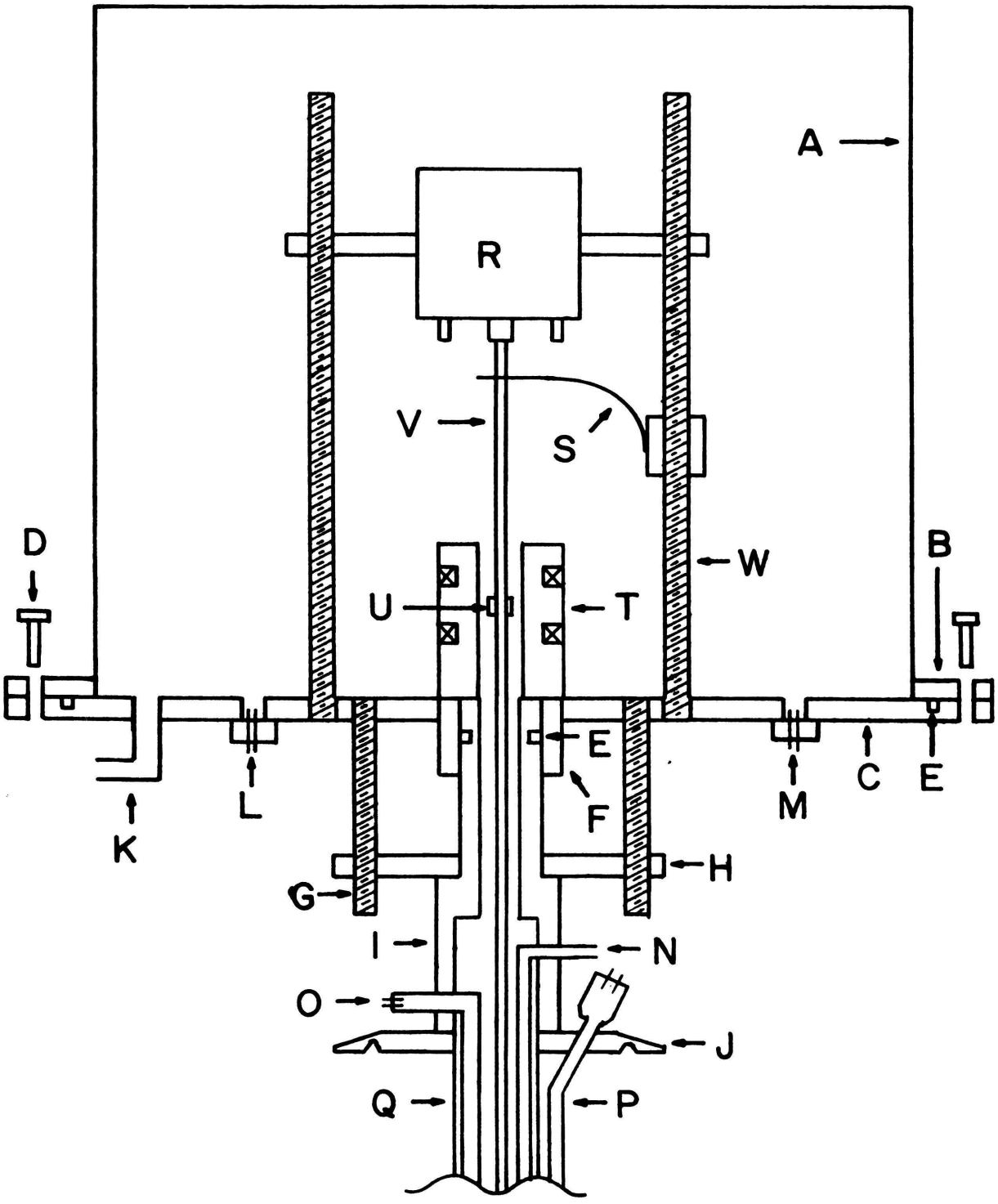

Figure 3

(G) both above and below the plate. (This design feature allows adjustment of the height of the base plate relative to the lower part of the magnetometer.) The bottom of sleeve (I) was silver soldered to a Ladish Triclover 3 inch flange (J) which serves to attach the magnetometer to the research insert dewar.

The atmosphere inside the magnetometer is adjusted through a copper tube (K) soldered to, and passing through, the base plate. A Veeco 1/4 inch value was soldered to (K). Electrical leads pass through the base plate by means of two brass plates (L and M) which incorporate electrical feed-throughs. The plates were vacuum sealed to the base plate by 'O'-rings.

Two 1/8 inch stainless steel tubes (N and O) pass through the side of sleeve (I) and extend downward inside the magnetometer from (I) to the vacuum furnace surrounding the sample. The tubes were soldered to (I) to provide a vacuum seal. The vacuum line for the furnace is denoted as (N). The electrical leads for the furnace pass through tube (O). A vacuum valve was soldered to (N) and an electrical feed-through was soldered to (O) outside (I) to provide a vacuum seal. A 1/8 inch stainless steel tube (P) passes through (J) and extends to the detection coil along the outside of the furnace support tube (Q). This tube contains the electrical leads to the detection coil. An electrical feed-through was soldered to (P) outside the research dewar to establish the vacuum seal of the insert dewar. A one inch stainless steel tube (Q) was silver soldered to (J) and extended from the magnetometer head at (J) to the vacuum furnace as a support.

The sample is forced to undergo sinusoidal displacement by a Pye-Ling vibration generator (Type V47, 30 ohm model). Figure 3 shows a representation of the driving mechanism mounted on the base plate (C). The generator (R) is mounted on a 1/4 inch thick aluminum plate by four 6-32 screws. The plate is supported above the base plate by four 1/4-20 threaded brass rods. The rods were screwed into and silver soldered to the base plate (C). Brass nuts on the 1/4-20 rods allow the height of the aluminum plate above the base plate to be adjusted. This allows a rough sample position adjustment which compensates for slight differences in sample driving rod lengths.

The vibration generator was not designed to support a large static load. Therefore a flat phosphor bronze static load spring is provided to support the static weight of the drive rod assembly. A representation of the spring is shown in Figure 3 (lettered as S). One end of the spring is attached to the drive rod just below the vibration generator. The other end is attached to a brass sleeve. The brass sleeve slips over one of the 1/4-20 bolts that support the vibration generator. Two 1/4-20 nuts were adjusted until the tension on the spring was sufficient to support the drive rod and sample.

A representation of the feedback coils (the gradient coil (T) and the reference coil (U)) is shown in Figure 3. The gradient coil form was machined from a one inch diameter phenolic rod. The dimensions for the coil were calculated by the process described in the theory section. Each coil of the antiHelmholtz pair has

approximately 2700 turns of number 39 copper magnet wire. The pair of coils were balanced using an external ac magnetic field so that the signal induced in each coil was the same. The gradient coil was mounted on the base plate (C). The reference coil was machined from a 0.45 inch diameter phenolic rod. It has approximately 990 turns of number 39 copper magnet wire. The reference coil was mounted on the threaded portion of the drive rod at the center of the gradient coil. Two nylon nuts clamp the reference coil in position.

B. Drive Rod and Sample Mount

Oscillatory motion is transmitted to the sample from the vibration generator by the drive rod (lettered as V in Figure 3). The drive rod is composed of a five inch length of 6-32 thread brass rod, a 3/16 inch diameter thin wall stainless steel tube, and 20 centimeters of 3 mm quartz tube. The 6-32 rod threads into the vibration generator. A 6-32 nylon nut tightened against the generator prevents the 6-32 rod from turning during operation. The static load spring is clamped to the 6-32 rod with nylon nuts. The 6-32 rod was screwed into a threaded brass sleeve which was soldered inside the 3/16 inch diameter stainless steel tube. The stainless steel tube extends from the magnetometer head down through the one inch diameter stainless steel furnace support tube (lettered as Q in Figure 3) to the junction with the quartz tube. The junction of the stainless steel tube and the quartz tube is far enough away from the detection coil so that any magnetization of the stainless

steel tube is very small compared to that of the sample. The quartz tube was attached to the stainless steel tube with epoxy. The quartz extends into the furnace and attaches to the sample holder.

The sample holder is a cylinder of boron nitride. A cross-sectional view of the sample holder is shown in Figure 4. Boron nitride is nonmagnetic and does not outgas in the required temperature range. A 3 mm hole was drilled in the top of the sample holder into which the quartz tube fits. A 0.110 inch hole was drilled through the sample holder perpendicular to its axis at the bottom of the 3 mm hole. The exposed end of the quartz tube was heated until it was soft by a hydrogen-oxygen mini-torch. The quartz tube was then compressed against the boron nitride sample holder. The softened quartz flowed into the 0.110 inch hole and when cooled, firmly attached the sample holder. A 0.110 inch hole was drilled axially into the bottom of the sample holder. The 0.100 inch diameter sample fits into this hole and is held in place by a boron nitride plug. The plug is pinned to the sample holder with a transverse length of copper wire which penetrates both the wall of the sample holder and the plug. A Chromel-Alumel thermocouple was mounted on the sample holder with its junction in contact with the sample. The thermocouple leads extend along the drive rod to the magnetometer head and out to the recorder through plate (L).

C. Vacuum Furnace

A cross-sectional view of the lower end of the magnetometer is

Figure 4. Cross-Sectional View of Sample Holder

1. 3 mm Quartz Tube (Drive Rod)
2. 0.110 Inch Hole with Quartz Constraints
3. Sample Position
4. Hole for Wire Pin
5. Boron Nitride Plug
6. Thermocouple

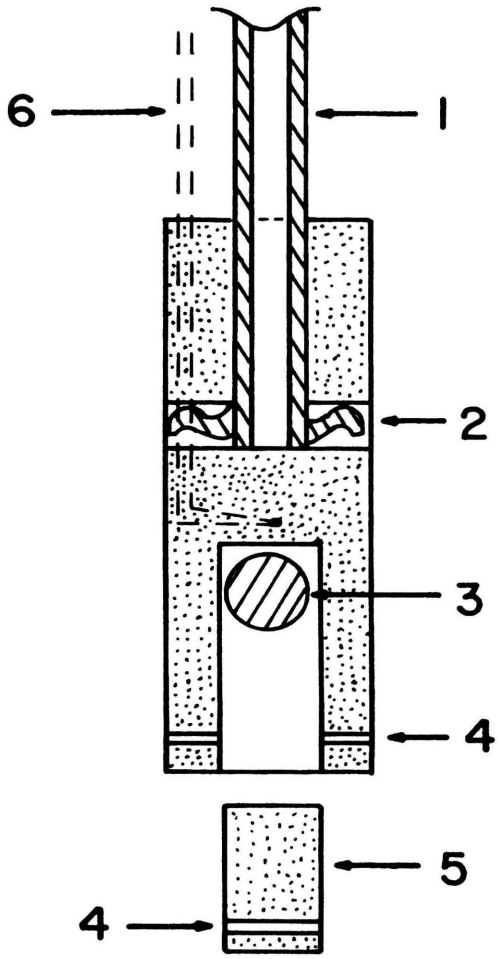

Figure 4

shown in Figure 5. The inner wall of the furnace is a 1/4 inch stainless steel tube. The bottom end of the tube was welded shut with a stainless steel cap. The other end was silver soldered to the brass coupling. The brass coupling was silver soldered to the one inch diameter stainless steel furnace support tube (Q in Figure 3). The two stainless steel tubes carrying the vacuum line and the electrical leads for the furnace were silver soldered to the brass coupling. These tubes extend from the magnetometer head to the furnace vacuum space. The outer vacuum jacket of the furnace is composed of a one inch diameter stainless steel tube stepped down to a 5/8 inch diameter stainless steel tube. The jacket was slipped over the furnace and soft soldered to the brass coupler. This outer jacket is easily removed for repair of the furnace heating element.

The outer surface of the 1/4 inch furnace tube was first roughed with a sandblaster. Then a thin layer of ceramic glaze was baked on the surface. Number 29 Nichrome wire was bifilar wound directly over the glazed tube, two inches to either side of the sample position. A thin layer of Alumina cement (C60 from the Thermal American Fused Quartz Co.) was spread over the wire and heat-treated with a propane torch. This cement had to be kept thin to avoid contact with the radiation baffles. The Alumina cement does not outgas nor become conductive within the temperature range required. Copper electrical leads were silver soldered to the Nichrome wire.

Figure 5. Cross-Sectional View of Lower End of Magnetometer

1. Brass Joint
2. Vacuum Line
3. Inner Furnace Wall
4. Outer Furnace Jacket
5. Spring Fingers
6. Furnace Heating Element
7. Detection Coil Assembly
8. Sample Position
9. Outer Radiation Baffle
10. Inner Radiation Baffle

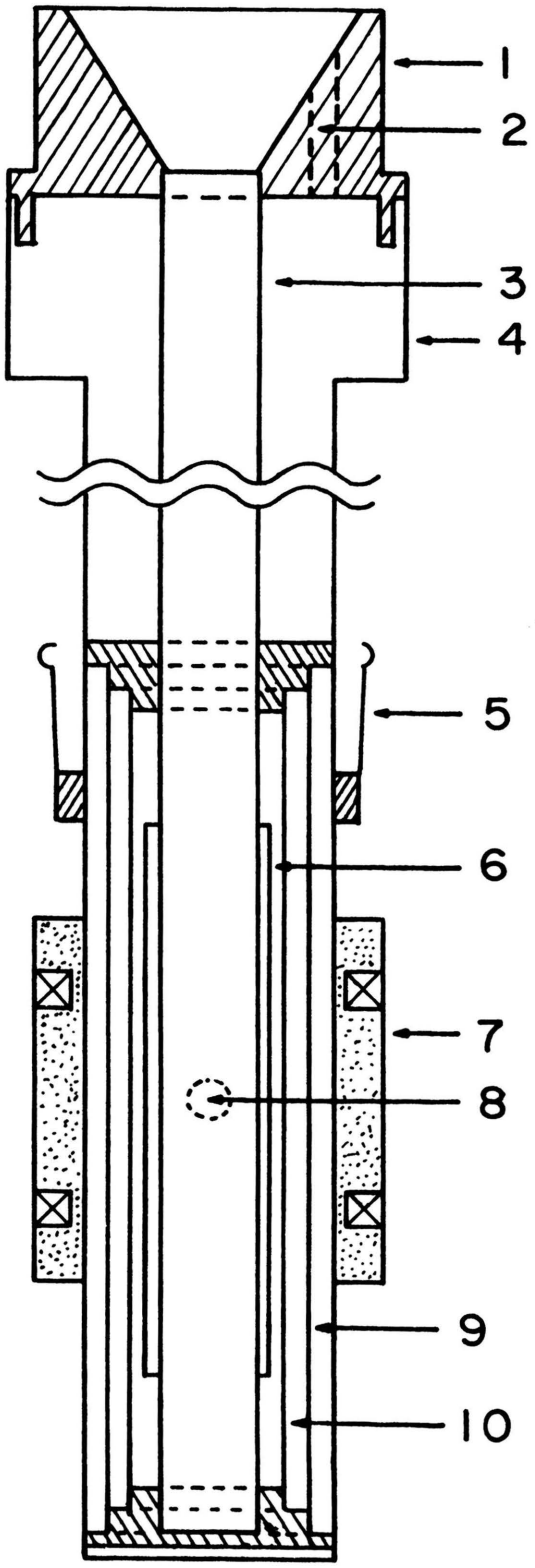

Figure 5

Two radiation baffles were used with the furnace: a 3/8 inch diameter and a 1/2 inch diameter stainless steel tube. The placement of the baffles are shown in Figure 5. A narrow lengthwise slit was made on each baffle to reduce the possibility of any eddy current shielding of the oscillating quadrupole signal. They were held in place and electrically insulated from the 1/4 inch tube by two Teflon sleeves, one at each end.

It is necessary that the furnace leak very little heat into the detection coil since the impedance of the coil is temperature dependent. Two types of energy loss had to be considered: thermal conduction and thermal radiation. In Figure 6 the performance of the vacuum furnace with two radiation baffles is compared to several other furnace designs. Curve A shows the result of pumping a furnace without radiation baffles to about 25 microns pressure. The thermal radiation becomes the major factor of power loss at high temperatures. Curve B shows the result of filling the furnace volume with Vermiculite at atmospheric pressure. The thermal radiation loss is not as sharp as in Curve A but the thermal conduction is now greater. The result of a combination of Vermiculite and reduced pressure of 25 microns is shown in Curve C. Higher temperatures with less power are obtained as expected. Curve D shows the result for the vacuum furnace with the two radiation baffles. The pressure in the furnace volume was about 10^{-5} Torr. A temperature of 1000° K was obtainable with 27 watts heater power. This system of radiation baffles and low pressure is similar to the design

Figure 6. Temperature Versus Power for Various Furnace Insulations

A. Fore Pump Vacuum

B. Vermiculite in Air

C. Vermiculite Under Fore Pump Vacuum

D. Double Radiation Baffles Under 10^{-5} Torr Vacuum

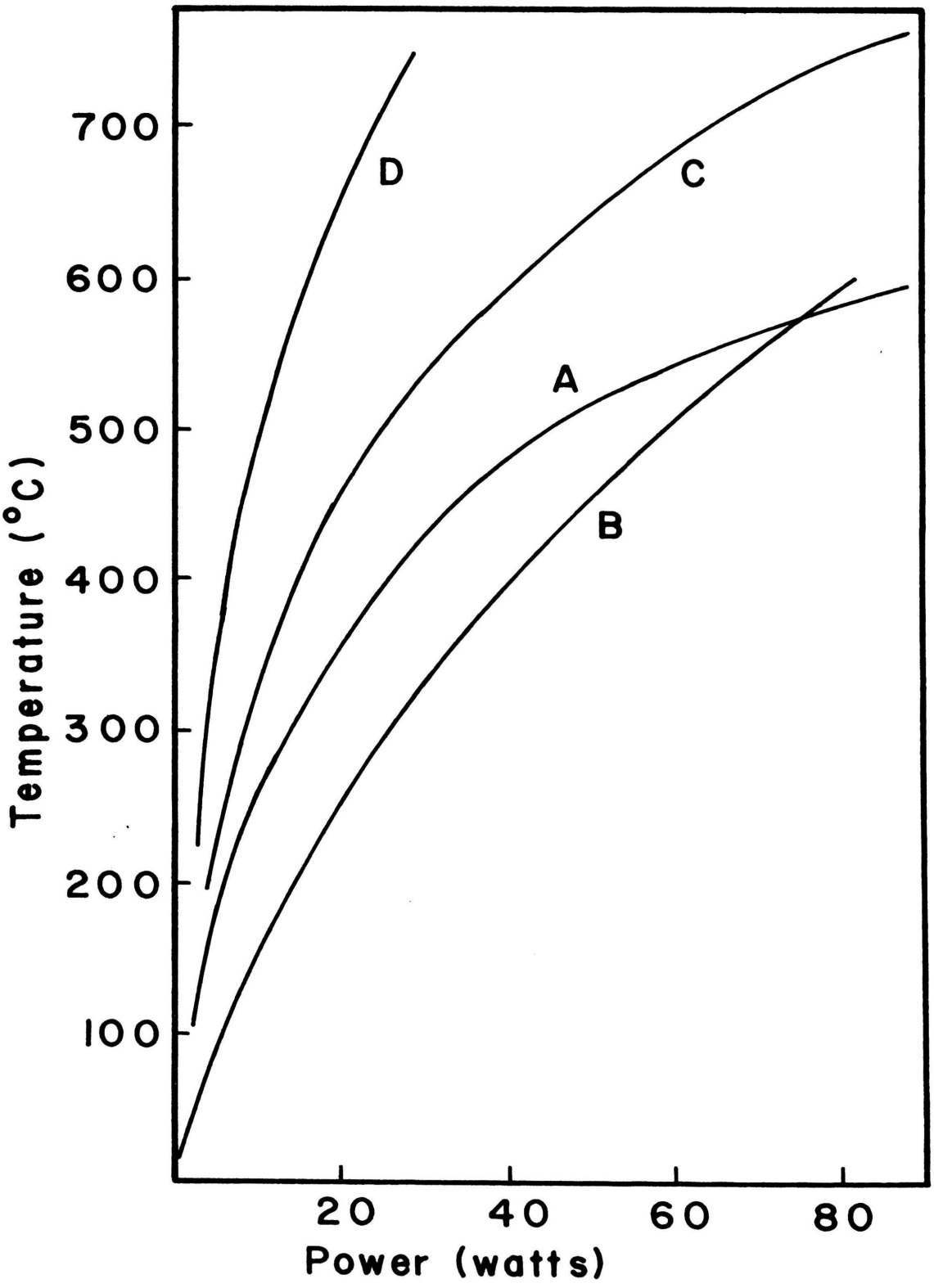
700
600
500
400
300
200
100
Temperature (°C)
D
C
A
B
20
40
60
80
Power (watts)

Figure 6

of the commercial PAR magnetometer furnace which attains 1050^{o} K at 25 watts.

D. Detection Coil

The dimensions for the detection coil were calculated by the process described in the theory section (reference 3). The outer diameter of the coil was limited to one inch by the I.C. of the insert dewar placed inside the superconducting solenoid. The inner diameter was limited to 5/8 inch by the outer diameter of the furnace jacket. The coil form was made from one inch diameter phenolic. Number 39 copper magnet wire was wound in square grooves so that each coil had approximately 1025 turns. The two coils were balanced in an external ac magnetic field so that the signal induced in each coil was the same.

The detection coil was tested to determine the required accuracy of the sample placement in its center. The output voltage of the detection coil versus sample position in the coil was plotted. Figure 7 shows the result of using a small piece of permanent magnet as the sample oscillating at 100 cps. The relative position of the sample with respect to the detection coil was changed by moving the coil along the outside of the furnace jacket. The flat region at the peak of the curve is approximately 6 mm wide with less than 1% change in output voltage. This result shows that the accuracy of the placement of the sample in the center of the detection coil is not a major problem.

In order to reduce motion of the detection coil in the external magnetic field, a brass sleeve with phosphor bronze spring fingers

Figure 7. Detection Coil Voltage Versus Relative Position of Sample

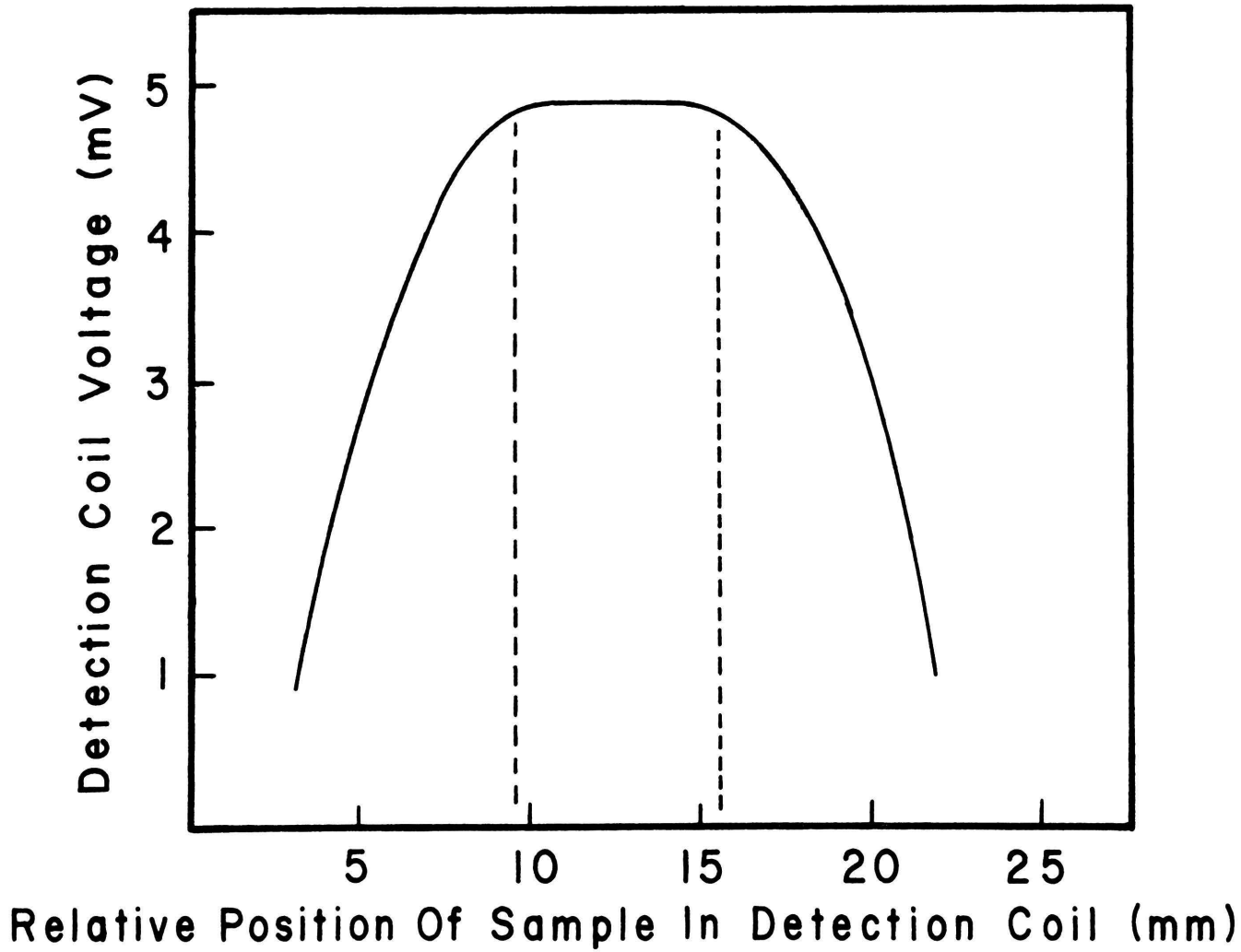
Detection Coil Voltage (mV)
5
4
3
2
1
5
10
15
20
25
Relative Position Of Sample In Detection Coil (mm)

Figure 7

was silver soldered to the furnace jacket above the position of the detection coil. The spring fingers fit tightly against the inner wall of the insert dewar.

E. Electronics

A PAR Model HR-8 lock-in amplifier was the basic electronic component of this magnetometer. This instrument provided a variable frequency and amplitude ac signal which was stable to one part in ten to the fourth. This signal was amplified by a Bogen Model M0200A audio amplifier and applied to the Pye-Ling vibration generator. The maximum potential to the vibration generator at maximum output of the lock-in amplifier was 10 volts. When the feedback system was tested, it was necessary to use a PAR Model 123 zero offset accessory with the lock-in amplifier. This was to null the ac signal induced in the reference coil by the ac magnetic fringe field from the vibration generator. A PAR Type A preamplifier was used with the lock-in amplifier. This preamplifier had an input impedance of 1 Megohm which minimized the temperature dependence of the system gain arising from the temperature dependent impedance of the detection coil. The lock-in amplifier amplified the signal from the magnetometer and converted the ac signal to a dc output voltage. This output voltage could be read directly or could be used in the feedback system. For materials with large magnetizations the dc output was insufficient to directly drive the feedback system. A booster amplifier was then placed between the lock-in amplifier and the feedback system.

The dc output of the lock-in amplifier was fed directly into an x-y recorder. The calibration of the magnetometer was amplitude and frequency dependent when the feedback system was not used.

V. RESULTS

A. Frequency Dependence

It was desirable to omit the feedback system for simplicity of operation, and instead, to test the possibility of using the dc output of the lock-in amplifier as a direct measure of the magnetization of the sample. This raised the question of what frequency and amplitude to use. A test was made to determine the frequency dependence of the output at constant driving voltage. It was found that with five volts ac across the vibration generator, the dc output from the lock-in amplifier decreased almost linearly with increasing frequency over the range of 60-200 cps. There was a mechanical resonance in the range of 20-40 cps. It was decided to use 100 cps as the measuring frequency.

B. Experimental Procedure

The superconducting solenoid was mounted in its dewar and the insert dewar was placed in the core of the solenoid. The solenoid and the two dewars were precooled to liquid nitrogen temperature. After the solenoid had been thoroughly cooled, the nitrogen was blown out and liquid helium was transferred into the solenoid dewar. A sample was mounted in the magnetometer and the inside of the magnetometer was evacuated by a force pump. It was then flushed with helium gas several times to remove other gases so that they did not freeze and impair the sample motion during low temperature operation. The vacuum shield surrounding the furnace was evacuated to 10^{-5} Torr by a diffusion pump and

sealed. The lower end of the magnetometer was precooled in liquid nitrogen in an external dewar, then the magnetometer was placed in the insert dewar. Liquid nitrogen was pumped into the insert dewar until it covered the detection coil. A carbon resistor, placed above the detection coil, was used as a liquid nitrogen level detector.

An ice bath was used as the reference point for the Chromel-Alumel thermocouple that measured the sample temperature. The temperature was read on a potentiometer in millivolts and a standard table for the Chromel-Alumel thermocouple was used to convert the millivolt readings to degrees centigrade. The dc output of the lock-in amplifier was connected to the y-axis of a x-y recorder and the power supply of the superconducting solenoid was connected to the x-axis. The x-y recorder plotted the magnetization (in volts) versus the external magnetic field (the solenoid current).

Current was supplied to the furnace by a dc constant current power supply. To decrease the temperature of the sample, the dc power supply was turned off. The temperature of the sample could be reduced more rapidly by poisoning the furnace vacuum with helium gas, but the furnace had to be pumped down to 10^{-5} Torr before current was supplied to the furnace again.

The frequency and amplitude were set to the calibration values on the lock-in amplifier. The external magnetic field was turned on and the sample position was adjusted to obtain the

maximum output signal from the detection coil. The phase control on the lock-in amplifier was adjusted for maximum output and the time constant of the lock-in was selected. The desired temperature of the sample was set by adjusting the dc current of the furnace. Once the desired temperature was reached, a multi-speed gear motor was used to slowly sweep the magnetic field. The magnetization versus magnetic field was plotted on the x-y recorder. The speed of the magnetic field sweep had to be slow enough so that the electronic components and recorder did not lag the actual output signal of the detection coil. If magnetization versus temperature at constant field was to be measured, the field was held constant, the thermocouple leads were connected to the x-axis of the recorder, and the temperature was swept.

After measurements for the standard sample were completed, a new sample of unknown magnetization was mounted in the magnetometer. While the standard sample was being removed, the temperature of the sample region had to be held between 0° C and room temperature to keep air from freezing in the sample region. After the new sample was mounted, the inside of the magnetometer was pumped and flushed with helium gas and measurements were made. If more samples were to be measured, the same procedure as above had to be followed. Liquid helium loss was remarkably small during the sample change.

C. Calibration

The magnetometer was calibrated using a single crystal of nickel as the standard sample. The nickel sample was first cut

into a 0.125 inch cube on a spark cutter. This cube was then ground to less than 1% out of round with a tumble type sphere grinder. Twenty random measurements of the diameter were made to determine the average diameter of the (near) sphere. The average diameter was 0.109 inch and the mass of the sample was 0.100 gm.

Figure 8 shows the dc output from the lock-in amplifier versus magnetic field for the nickel calibration sample. The frequency of vibration was 100 cps. The reference attenuation on the lock-in amplifier was 0.05. The voltage sensitivity was 20 mV. The time constant of the lock-in was 1 second/6 db. The temperature of the sample was -23° C. The detection coil was not immersed in liquid nitrogen.

The initial slope and the saturation line were extrapolated to intersection. The value for the magnetic field at the intersection of these two lines was 2.05 kilogauss. Using equation 27 with N = 1/3,

$$4\pi M_s = 6.15 \text{ kilogauss}, \tag{28}$$

where M_s has the units of emu per unit volume. To convert the value of M_s so that it has the units of emu per gram, M_s was divided by the density of the sample. Using 8.90 gms/cm^3 as the density[29], M_s in emu/gm was

$$M_s = 54.7 \text{ emu/gm}. \tag{29}$$

Figure 8. Nickel Calibration Curve: Magnetization Versus External Field

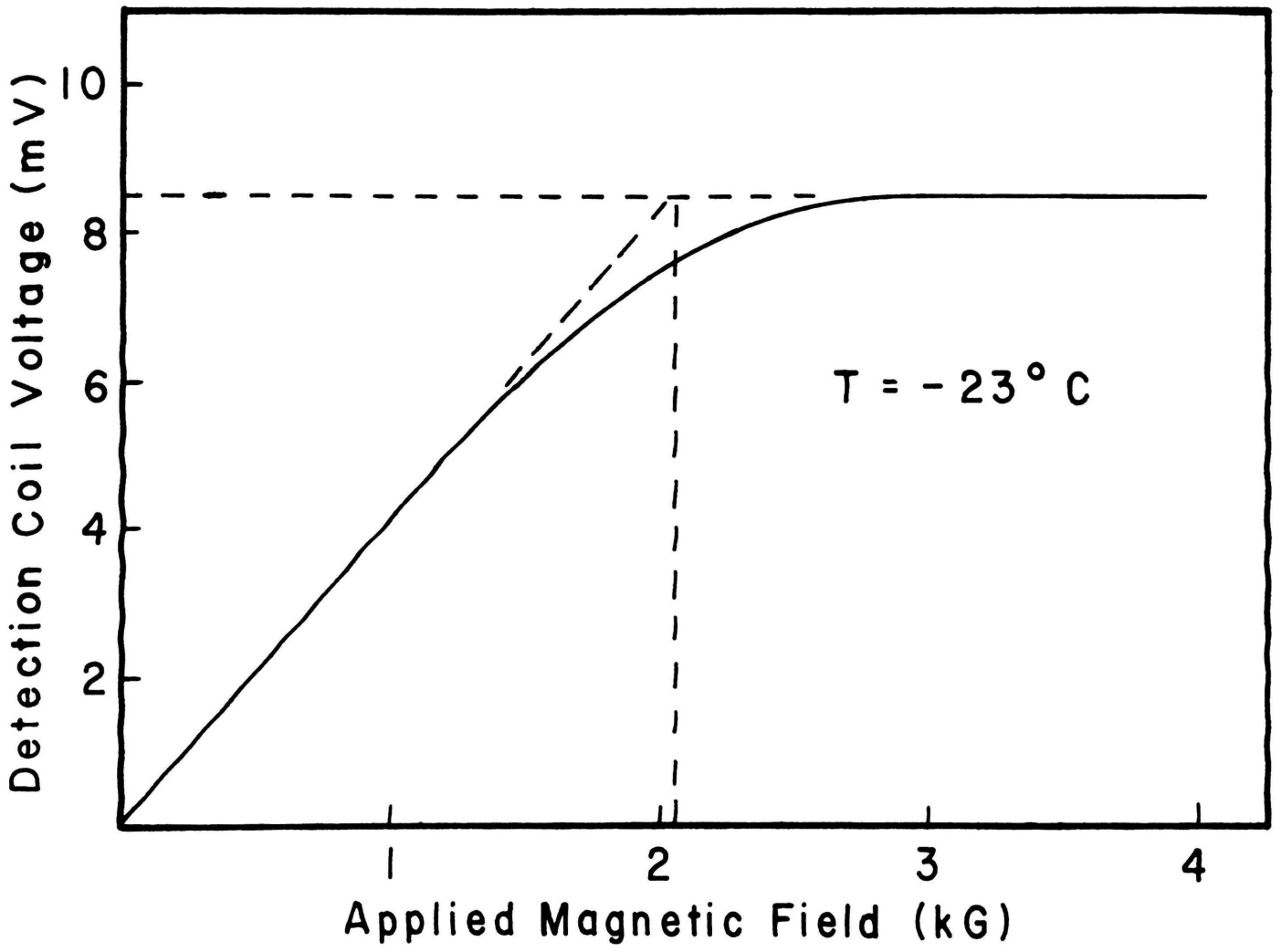
Detection Coil Voltage (mV)
10
8
6
4
2
T = - 23° C
1
2
3
4
Applied Magnetic Field (kG)

Figure 8

Reference 29 quoted several values for M_s that ranged from 54.3 to 55.5 emu/gm at temperatures that ranged from 15° C to room temperature. Equation 29 could not directly be compared to those values since they were at different temperatures, although equation 29 was within 0.4% of the average reported magnetization of nickel.

Figure 9 shows the magnetization versus temperature at constant field for the nickel sample. The thermocouple leads were directly connected to the x-axis and the external field was 10 kilogauss. (This was well above the saturation field). The frequency of vibration was 100 cps. The reference attenuation of the lock-in amplifier was 0.05. The voltage sensitivity was 20 mV. The time constant of the lock-in was 1 second/12 db. The detection coil was immersed in liquid nitrogen to stabilize the temperature of the detection coil. The thermocouple was calibrated at liquid nitrogen temperature. The Curie temperature shown on Figure 9 was only a few degrees different from the quoted Curie temperature of nickel (358° C).

Equation 29 was compared to the literature values for M_s by using the results shown on Figure 9. The voltage reading that corresponded to -23° C from Figure 9 was equated to equation 29 which resulted in a emu per gram per millivolt constant (K).

$$K = 3.80 \text{ emu}/(\text{gm}\cdot\text{mV}). \tag{30}$$

The voltage reading that corresponded to 20° C from Figure 8 was

Figure 9. Nickel Calibration Curve: Magnetization Versus Sample Temperature

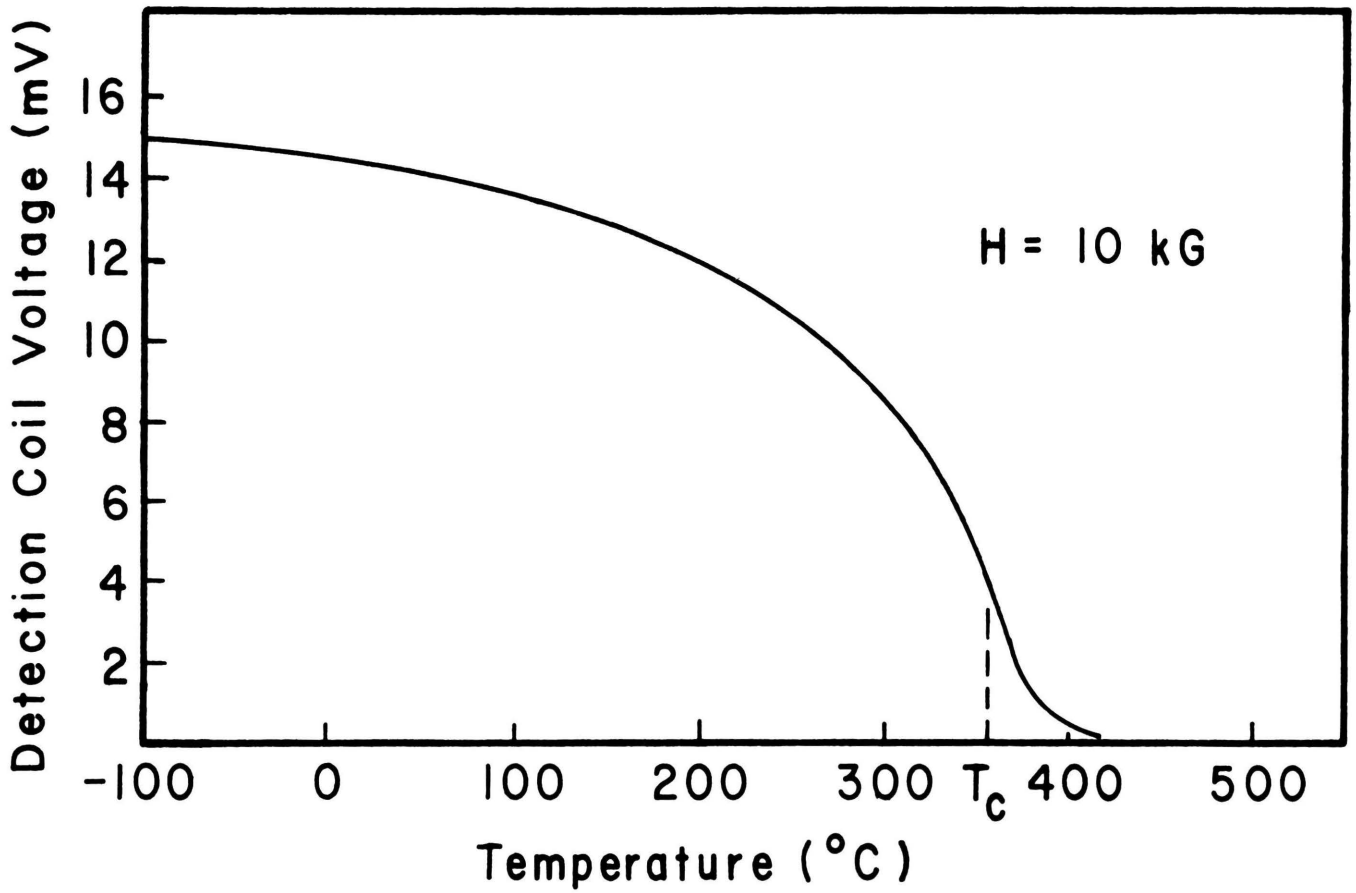
Detection Coil Voltage (mV)
16
14
12
10
8
6
4
2
H = 10 kG
-100
0
100
200
300
T_c
400
500
Temperature (°C)

Figure 9

multiplied by this constant to give the magnetization in emu per gram at this temperature.

$$M_s(20^{\circ}\ C) = 54.4\ \text{emu/gm}. \qquad (31)$$

Reference 29 gave the value of 54.6 emu/gm at 20° C in a field of 8 kilogauss. That was a 0.37% error compared to equation 31. Another value for M_s given in reference 29 was 55.1 emu/gm at 15° C. The field was extrapolated to infinite field. That was a 1.3% error compared to equation 31. The values at 15° C and at 20° C were indistinguishable from each other on Figure 9.

VI. CONCLUSIONS

During the course of this research it was found that a pursuit of the best design parameters for the vibrating sample magnetometer led time and time again to a very close copy of the Princeton Applied Research version of the Foner magnetometer. While the total price for the construction of this instrument was approximately one eigth that asked by P.A.R., the development time approximated three years. What was saved in capital cost was paid in extended development time.

Calibration by either the slope method or by comparison with a standard sample agreed to within one percent (nickel standard). It is important that the reference sample show good saturation in order that M_s be fully realized. The slope method is less satisfactory when the sample is badly strained, since the linear portion of the initial magnetization is greatly abbreviated in that case.

This thesis research is now concluded with the realization of a vibrating sample magnetometer matching or exceeding the performance of the P.A.R. machine. Temperature calibration is within two degrees at 400° C, and the magnetization calibration is within one percent for spherical samples.

BIBLIOGRAPHY

1. Estermann, Immanuel, editor, Methods of Experimental Physics: Classical Methods, Academic Press, New York, 1959, Page 536.

2. Arrott, Anthony, and J. E. Goldman, Rev. Sci. Instr. 28, 99 (1957).

3. Zijlstra, H., Experimental Methods In Magnetism, Vol. IX, No. 1 and 2, John Wiley and Sons, Inc., New York, Page 29 (1967).

4. Foner, S., Phys. Rev. 101, 1648 (1956).

5. Holder, B. E., and M. P. Klein, Phys. Rev. 98, 265(A) (1955).

6. Seavey, M. H., Jr., and P. E. Tannenwald, J. Appl. Phys. 29, 292 (1958).

7. Bates, L. F., Modern Magnetism, Cambridge University Press, New York, 1963, Pages 122-124.

8. Bates, Pages 115-118.

9. Smith, D. O., Rev. Sci. Instr. 27, 261 (1956).

10. Dwight, K., N. Menyuk, and D. Smith, J. Appl. Phys. 29, 491 (1958).

11. Flanders, P. J., Proceedings of the Conference on Magnetism and Magnetic Materials, Boston, 1956, AIEE Spec. Publ. T-91, Page 388.

12. Lubell, M. S., and A. S. Venturino, Rev. Sci. Instr. 31, 207 (1960).

13. Foner, Simon, Rev. Sci. Instr. 30, 548 (1959).

14. Foner, S., and E. J. McNiff, Jr., Rev. Sci. Instr. 39, 171 (1968).

15. Richards, D. B., L. R. Edwards, C. M. Cornforth, and S. Legvold, Rev. Sci. Instr. 41, 647 (1970).

16. Case, W. E., and R. D. Harrington, J. Research, National Bureau of Standards, Vol. 70C, No. 4, 255 (1966).

17. Bates, Pages 136-137.

18. Plotkin, H., Quart. Progr. Rept. Massachusetts Institute of Technology Research Lab. Electronics (October 15, 1951), Page 28.

19. Foner, S., Rev. Sci. Instr. 27, 548 (1956).

20. Noakes, J. E., A. Arrott, and C. Haakana, Rev. Sci. Instr. 39, 1436 (1968).

21. Princeton Applied Research Bulletin, "Magnetometers for Materials Susceptibility Research", 1970.

22. Cross, P. H., Rev. Sci. Instr. 32, 1179 (1961).

23. Bond, W. L., Rev. Sci. Instr. 22, 344 (1951).

24. Bond, W. L., Rev. Sci. Instr. 25, 401 (1954).

25. Experimental Methods In Magnetism, Pages 42-46.

26. Bates, Page 65.

27. Case, Page 261.

28. Case, Page 259.

29. Case, Page 257.

VITA

Donald Dwight Hoffman was born on August 24, 1946, in Abilene, Kansas. He received his primary education at Rural Center Grade School and his secondary education at Chapman, Kansas. He received his college education from Kansas Wesleyan University, in Salina, Kansas, from which he received a Bachelor of Arts in Physics in May 1968.

He has been enrolled in the Graduate School of the University of Missouri at Rolla since August 1970 and has held the National Defense Education Act Fellowship for the period August 1970 to August 1973.